Adapting genotyping-by-sequencing and variant calling for heterogeneous stock rats

Jianjun Gao[*⁋], Alexander F. Gileta[* †⁋], Hannah V. Bimschleger[*], Celine L. St. Pierre[*], Shyam Gopalakrishnan[#], Abraham A. Palmer[*‡]

* Department of Psychiatry, University of California San Diego, La Jolla, California, 92093

† Department of Human Genetics, University of Chicago, Chicago, Illinois, 60637

Natural History Museum of Denmark, University of Copenhagen, 1350 København K, Denmark

‡ Institute for Genomic Medicine, University of California San Diego, La Jolla, California, 92093

⁋ These authors contributed equally to this work.

Running title: GBS and variant calling in HS rats

Key words: genotyping-by-sequencing, heterogeneous stock, rat, imputation

Corresponding author: Abraham A. Palmer

Mailing address: 9500 Gilman Drive #0667, La Jolla, CA, 92093

Phone number: 858-534-2093

Email: aapalmer@ucsd.edu

ABSTRACT

The heterogeneous stock (**HS**) is an outbred rat population derived from eight inbred rat strains. The population is maintained with the goal of minimizing inbreeding and maximizing the genetic diversity of the stock. Only a few genotyping microarrays have been created for rats; they were expensive and are no longer in production. To obtain high-density genome-wide marker data for genetic mapping, we have adapted genotype-by-sequencing (**GBS**) for use in rats. Herein, we outline the laboratory and computational steps we took to optimize an efficient double digest genotype-by-sequencing (**ddGBS**) protocol for rats. To analyze the ddGBS sequencing data, we evaluated multiple existing computational tools and designed a workflow that allowed us to call and impute over 3.7 million SNPs genome-wide in the HS. We also compared various rat genetic maps for use in imputation, including a recently developed map specific to the HS. Using the pipeline, we obtained concordance rates of 99% with data from a rat genotyping array. The computational pipeline that we have developed could be easily adapted for use in other species. We include a detailed protocol to perform ddGBS in rats.

INTRODUCTION

Advances in next-generation sequencing technology over the past decade have enabled the discovery of high-density, genome-wide single nucleotide polymorphisms (**SNPs**) in model systems. Comprehensive assays of the standing genetic variation in these organisms has allowed for the identification of quantitative trait loci and the application of numerous population genetic and phylogenetic methods. However, due to the linkage disequilibrium (**LD**) structure in many structured breeding populations, sequencing the whole genome is not necessary. SNPs are frequently in strong LD with adjacent loci, effectively 'tagging' nearby variation, and thereby reducing the number of sites that need to be genotyped. Several reduced-representation

sequencing approaches that take advantage of LD structure have been previously described (Miller et al. 2007; van Orsouw et al. 2007; Van Tassell et al. 2008; Baird et al. 2008; X. Huang et al. 2009; Davey et al. 2011; Elshire et al. 2011; Poland et al. 2012; Peterson et al. 2012; Sun et al. 2013; Scheben, Batley, and Edwards 2017). Thousands of SNPs can be identified in large numbers of samples for a fraction of the price of other genotyping methods (Chen et al. 2013; He et al. 2014). The advantages of these methods are especially attractive when considering genotyping less commonly utilized species or strains for which genotyping microarrays are not available.

Of the existing reduced-representation protocols, the genotyping-by-sequencing (**GBS**) approach developed by Elshire et al. (Elshire et al. 2011) has been frequently modified to accommodate non-model species, such as: soybean (Sonah et al. 2013), rice (Furuta et al. 2017), oat (Fu and Yang 2017), chicken (Pértille et al. 2016; Wang et al. 2017), mouse (Parker et al. 2016), fox (Johnson et al. 2015), and cattle (De Donato et al. 2013), among others. The greatly varying genomic composition among organisms necessitates a diverse and customized set of approaches for obtaining high-quality genotypes. As such, both the GBS protocol and computational pipeline require modification when being applied to a new species. Recent work from our group showed that GBS can be effectively applied to outbred mice (Parker et al. 2016; Gonzales et al. 2017; Zhou et al. 2018) and rats (Fitzpatrick et al. 2013). However, those publications used protocols that had not been optimized, leaving significant room for improvement in genotype quality and marker density. Additionally, although several tools and workflows for the analysis of GBS data have been described, including: stacks (Catchen et al. 2013), IGST-GBS (Sonah et al. 2013), TASSEL-GBS (Glaubitz et al. 2014), Fast-GBS (Torkamaneh et al. 2017), and GB-eaSy (Wickland et al. 2017), the majority were developed and optimized for use in plant

species and given the lack of well-developed genomic resources in these species, do not include an imputation step.

The HS is an outbred rat population created in 1984 using eight inbred strains and has been maintained since then with the goal of minimizing inbreeding and maximizing the genetic diversity of the colony (Johannesson et al. 2008; Woods and Mott 2017). After more than 80 generations of accumulated recombination events, their genome has become a fine-scale mosaic of the inbred founders' haplotypes. The breeding scheme and the number of accumulated generations has made the HS colony attractive for genetic studies. Additionally, extensive deep sequencing data exists for the eight progenitor strains, allowing for accurate imputation from sites directly captured by GBS to millions of additional SNPs.

Detailed here are the steps we have taken to optimize a rat GBS protocol and computational pipeline. Drawing on existing protocols (Elshire et al. 2011; Peterson et al. 2012; Poland et al. 2012; Parker et al. 2016) as models, we redesigned our GBS approach and have developed a novel, reference-based, high-throughput workflow to accurately and cost-effectively call and impute variants from low-coverage double digest GBS (**ddGBS**) data in rats. This publication is intended as a resource for other who might wish to perform GBS in rats and should also be helpful for adapting GBS for use in new species. We demonstrate that with a suitable reference panel, applying reduced representation approaches and imputation in model systems can provide high-confidence genotypes on millions of genome-wide markers.

MATERIALS AND METHODS

Tissue samples and DNA extraction

Samples for this study originated from three sources: an inhouse advanced intercross line (**AIL**) derived from LG/J and SM/J mice (Gonzales et al. 2018), Sprague Dawley (**SD**) rats from Charles River Laboratories and Harlan Sprague Dawley, Inc. (Gileta et al. 2018), and an HS rat colony (Woods and Mott 2017; Chitre et al. 2018). Early ddGBS optimization utilized AIL genomic DNA extracted from spleen by a standard salting-out protocol. Later optimization steps were performed using genomic DNA from SD rats extracted from tail clippings using the PureLink Genomic DNA Mini Kit (Thermo Fisher Scientific, Waltham, MA). Optimization of the ddGBS sequencing data analysis pipeline was performed on various subsets of our final sample of 4,973 HS rats. HS rat DNA was extracted from spleen tissue using the Agencourt DNAdvance Kit (Beckman Coulter Life Sciences, Indianapolis, IN). All genomic DNA quality and purity was assessed by NanoDrop 8000 (Thermo Fisher Scientific, Waltham, MA). Interestingly, we have observed that rat genomic DNA appears to degrade faster than mouse genomic DNA following extraction; therefore, we recommend storing rat genomic DNA at -20° and using it within months of extraction whenever possible.

In silico digest of rat genome

We used *in silico* digests to aid in the selection of restriction enzymes, with the goal of maximizing the portion of the genome captured at sufficient depth to make confident genotype calls. Increasing the proportion of the genome covered assists with fine-mapping. The rn6 rat genome assembly was downloaded in FASTA format from UCSC (Kent et al. 2002). We used the *restrict* function within EMBOSS (version 6.6.0) (Rice, Longden, and Bleasby 2000) in conjunction with the REBASE database published by New England BioLabs (NEB; version 808) (Roberts and Macelis 1999) to perform *in silico* digest of rn6. We performed the digest with PstI alone and then with PstI paired with each of 7 secondary enzymes: AluI, BfaI, DpnI, HaeIII, MluCI, MspI, and NlaIII.

We only considered fragments with one PstI cut site and one cut site from the secondary enzyme because the adapter and primer sets are designed to only allow these fragments to amplify. The number of fragments with one of each of the cut sites were summed for all observed lengths and the results summarized in Figure 1 and Table 1.

Restriction Enzyme(s)	Recognition sequence	Length of Overhang (bp)	% Genome in 250-400bp Region+	% Genome in 300-450bp Region+
PstI	CTGCA^G	4	0.48%	0.56%
PstI + AluI	AG^CT	0	3.06%	2.88%
PstI + BfaI	C^TAG	2	3.10%	3.25%
PstI + DpnI*	GA^TC	0	2.69%	3.00%
PstI + HaeIII	GG^CC	0	2.71%	2.79%
PstI + MluCI	^AATT	4	3.32%	3.21%
PstI + MspI	C^CGG	2	1.16%	1.24%
PstI + NlaIII	CATG^	4	3.45%	3.31%

Table 1. Restriction enzyme options for double digest.

The percent genome in region columns indicate the percentage of the genome that falls within the provided fragment size ranges and can therefore be capture by GBS.

* Restriction enzyme is methylation sensitive.

+ Calculated using rn6 genome length of 2,870,182,909bps.

Figure 1. ***In silico*** **digest fragment distributions for PstI and potential secondary restriction enzymes.**

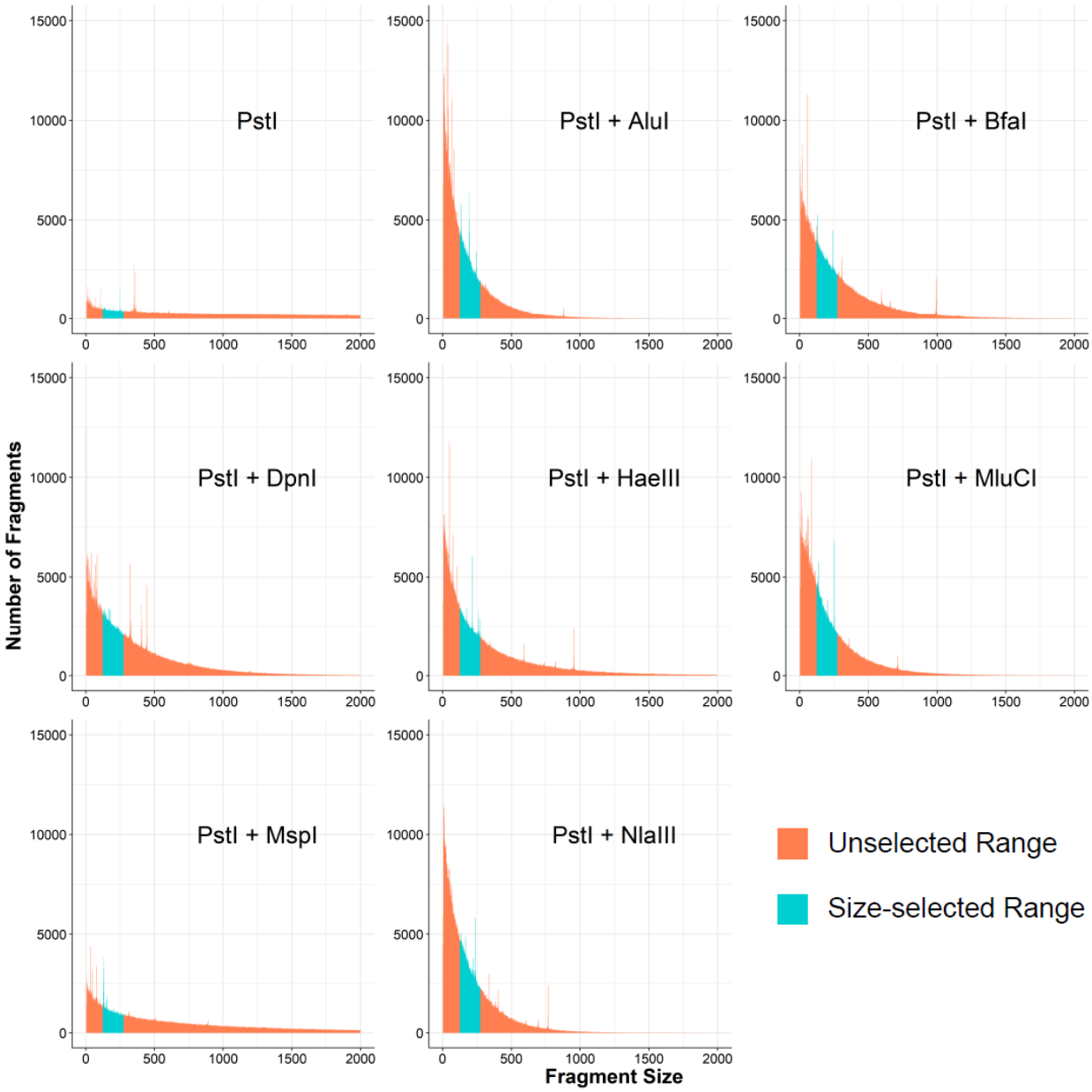

Each panel represents an independent digest of rn6 with the listed enzyme(s). Regions highlighted in blue are fragments that would be selected by the Pippin Prep (125-275bp) after annealing

adapters and primers. These regions are quantified in Table 1 by multiplying the length of the fragments by the number of fragments to estimate the portion of the genome captured.

Restriction enzyme selection

Initial criteria for selecting a secondary restriction enzyme were: a 4bp recognition sequence, no ambiguity in the recognition sequence (i.e. N's), compatible with the NEB CutSmart Buffer, and an incubation temperature of 37°C. The list of enzymes meeting these criteria at the time included: AluI, BfaI, DpnI, HaeIII, MluCI, MspI, and NlaIII. Using the *in silico* digest data, we looked to maximize the portion of the genome contained within a fragment size range of 125-275bp (250-400bp with annealed adapters and primers). We excluded enzymes that produced blunt ends, both because it would be more difficult to anneal adapters to blunt ended fragments and because our adapters would then also anneal to blunt ends produced by DNA shearing. We also excluded methylation-sensitive enzymes, as we did not want to limit the breadth of our sequencing efforts, accepting the possibility of read pileup in repetitive regions. Based on these criteria, NlaIII, BfaI, and MluCI were selected for further testing.

ddGBS library preparation and sequencing

The full ddGBS protocol is available in File S1. In brief, approximately 1µg of DNA is used per sample. Sample DNA, PstI barcoded adapters, and NlaIII Y-adapter are combined in a 96-well plate and allowed to evaporate at 37°C overnight. Sample DNA and adapters are re-eluted on day two with a PstI/NlaIII digestion mix and incubated at 37°C for two hours to allow for complete digestion. Ligation reagents are then added and incubated at 16°C for one hour to anneal the adapters to the DNA fragments, followed by a 30-minute incubation at 80°C to inactivate the

restriction enzymes. Sample libraries are purified using a plate from a MinElute 96 UF PCR Purification Kit (QIAGEN Inc., Hilden, Germany), vacuum manifold, and ddH_2O. Once re-eluted, libraries are quantified in duplicate with Quanit-iT PicoGreen (Thermo Fisher Scientific, Waltham, MA) and pooled to the desired level of multiplexing (i.e. 12, 24, or 48 samples per library). Pooled libraries are concentrated to obtain the desired volume for use in the Pippin Prep. The concentrated pool is quantified to ensure the gel cassette will not be overloaded with DNA (>5µg). The pool is then loaded into the Pippin Prep for size selection (300-450bps) using a 2% agarose gel cassette on a Pippin Prep (Sage Science, Beverly, MA). Size-selected libraries were then PCR amplified for 12 cycles to increase the quantity of DNA, concentrated, and checked for quality on an Agilent 2100 Bioanalyzer with a DNA 1000 Series II chip (Agilent Technologies, Santa Clara, CA)., Bioanalyzer results were used to assure sufficient DNA concentration and to identify excessive primer dimer peaks.

An initial 96 HS samples were sequenced, 12 samples per library, at Beckman Coulter Genomics (now GENEWIZ) on an Illumina HiSeq 2500 with v4 chemistry and 125bp single-end reads. Subsequently, we began using a set of 48 unique barcoded adapters (File S2) to multiplex 48 HS samples per ddGBS library. Each library was run on a single flow cell lane on an Illumina HiSeq 4000 with 100bp single-end reads at the IGM Genomics Center (University of California San Diego, La Jolla, CA).

Figure 2. ddGBS sequencing data analysis workflow. Each step of the workflow is described in the text.

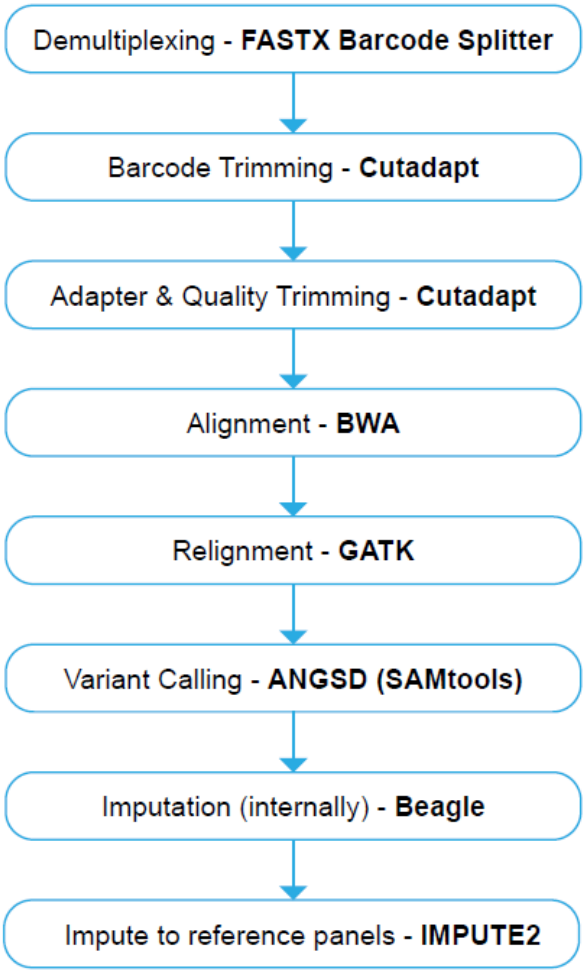

Evaluation of ddGBS pipeline performance

We present the steps required to call and impute genotypes from ddGBS data in Figure 2. During optimization of the pipeline, performance was assessed by two primary metrics: (1) the number of variants called and (2) genotype concordance rates for calls made in 96 HS rats that had both ddGBS genotypes and array genotypes from the Axiom MiRat microarray. After each step of the pipeline, the variant count and concordance rates were computed again. There were two checkpoints in the GBS pipeline where genotype quality (measured by concordance rate) was

assessed: after internal imputation within Beagle (Browning and Browning 2009, 2016) and again after imputation to the reference panel with IMPUTE2 (B. N. Howie, Donnelly, and Marchini 2009; B. Howie et al. 2012). A third, additional metric we checked was the transition to transversion ratio ($T_S T_V$), which is expected to be ~2.

Demultiplexing

The PstI adapter barcodes were used to demultiplex FASTQ files into individual sample files. Three demultiplexing software packages were tested: FASTX Barcode Splitter (Hannon Lab 2010), GBSX (Herten et al. 2015), and an in-house Python script (Parker et al. 2016). Input included the FASTQ files along with a plain text file containing samples identifiers, associated barcode sequences, and (if applicable) the name of the restriction enzymes used during library preparation. Reads that could not be matched with any barcode (1 mismatch was allowed), or that lacked the appropriate enzyme cut site, were discarded. Samples with less than two million reads after demultiplexing were removed. Data concerning demultiplexing shown in Table S1 are from a single HS rat sequenced in a 12-sample library on one lane after demultiplexing and adapter/quality trimming.

Barcode, adapter, and quality trimming

FASTQ read quality was assessed using FastQC v0.11.6 (Andrews 2017). We compared the efficacy of two rapid, lightweight software options for trimming barcodes, adapters, and low-quality bases from the NGS reads: Cutadapt (Martin 2011) and the FASTX Clipper/Trimmer/Quality Trimmer tools (Hannon Lab 2010) (Table S2). A base quality threshold of 20 was used and reads trimmed to below 25bps were discarded. Variant data was summarized using PLINK/SEQ (Purcell 2014).

Read alignment and indel realignment

Rattus norvegicus genome assembly Rnor_6.0 (rn6) was used as the reference genome for read alignment with the Burrows-Wheeler Aligner (BWA) (H. Li and Durbin 2009) using the *mem* algorithm. Using ANGSD to call variants from the aligned reads, we were able to compare variant counts at multiple mapping quality thresholds: 20, 30, 45, 60 and 90 (Table S3). We then used GATK IndelRealginer (McKenna et al. 2010) to improve alignment quality by locally realigning reads around a reference set of known indels in 42 whole-genome sequenced inbred rat strains, including the eight HS progenitor strains (Hermsen et al. 2015).

Variant calling and imputation

Variants were called using ANGSD v0.911, for which we employed the SAMtools model (Korneliussen, Albrechtsen, and Nielsen 2014; Durvasula et al. n.d.) followed by Beagle v4.1 (Browning and Browning 2009, 2016), which was used to impute missing genotypes at sites that had calls for only a subset of individuals (no reference panel was used). Prior to selecting ANGSD/Beagle, GATK's UnifiedGenotyper and HaplotypeCaller (McKenna et al. 2010) were tested with various parameter settings, but we did not obtain satisfactory performance. Using ANGSD, we inferred the major and minor alleles (*-domajorminor* 1) from the genotype likelihoods, kept only high confidence polymorphic sites (*-snp_pval* 1e-6), and estimated the allele frequencies based on the inferred alleles *(-domaf* 1). We discarded sites missing read data in more than 4% of samples (*–minInd*). Additionally, we tested altering thresholds for minimum base quality score (*-minQ*) and mapping quality (*-minMapQ*). Beagle also converted the ANGSD VCF file format to the more conventional VCF 4.1 format and phases genotype data.

QC and pre-phasing for reference panel imputation

Prior to imputing SNPs from the 42 inbred strain reference panel, we checked concordance rates for the 96 HS animals with array genotypes, examined the $T_S T_V$ ratio, and assessed whether the sex as recorded in the pedigree records agreed with the sex empirically determined by the proportion of reads on the X-chromosome out of the total number of reads (Figure S1). We also identified Mendelian errors using the --mendel option in *plink* and known pedigree information for 1,136 trios from 214 families within the HS sample. We looked at both Mendelian errors at the level of samples and at the level of SNPs. Using the fraction of the trios that were informative for a given SNP and the formula $1-(1-2p(1-p))^3$, where p represents the minor allele frequency of the allele, we formed curves for the distributions of the expected number of Mendelian errors for both SNPs and samples and chose the inflection points as thresholds. This approach filtered out 4 samples and 4,179 SNPs from subsequent analyses. Lastly, we only retained variants previously identified in the 8 HS founders (Ramdas et al. 2018) for use in imputation to the 42 genomes (Hermsen et al. 2015).

To improve imputation accuracy and computational efficiency, we employed a pre-phasing step prior to reference imputation. A flowchart outlining the pre-phasing protocol is presented in Figure S2. We tested three methods of converting genotype data to phased .hap files: VCFtools (--*impute*) (Danecek et al. 2011), SHAPEIT (Delaneau, Marchini, and Zagury 2011), and IMPUTE2 (*-prephase_g*) (B. N. Howie, Donnelly, and Marchini 2009). We assessed performance by checking genotype concordance rates for the 96 HS samples with array data.

Genetic maps

Genetic maps are required for proper phasing and imputation with IMPUTE2. When we began this project, no strain-specific recombination map was available for HS rats. Thus, we considered a sparse genetic map for SHRSPxBN (Steen et al. 1999). We also tested two types of linear (with

respect to physical distance) genetic "maps", which have recombination rates set at 1cM/Mb or the chromosome specific averages for rats, as reported by Jensen-Seaman et al. (Jensen-Seaman 2004). Lastly, late in the evolution of this project, we experimented with an HS-specific genetic map developed by Littrell et al. the Medical College of Wisconsin (Littrell et al. 2018).

Imputation to reference panel

We used existing sequencing and array data from the HS rat founder and other inbred laboratory rat strains (Hermsen et al. 2015) as reference panels for imputation. Genotype data underwent QC and were phased by Beagle into single chromosome haplotype files. Haplotype files were then created using the workflow detailed in Figure S2. Imputation by IMPUTE2 was performed in 5Mb chunks of the genome using the aforementioned reference panels and genetic maps. The chunks were subsequently concatenated by order of physical positions for each chromosome individually.

Data availability

Data Genotype data will be available at https://doi.org/10.6084/m9.figshare.7597697 and the code necessary to run the steps outline in the publication provided here https://doi.org/10.6084/m9.figshare.7597694. Additional data is available upon request.

RESULTS

ddGBS optimization

Previous projects utilizing GBS in mice and rats (Fitzpatrick et al. 2013; Parker et al. 2016; Gonzales et al. 2018) often encountered an issue where certain regions of the genome experienced high pileups of reads per sample (>100x), while other regions were covered by just 1-2 reads. This read distribution imbalance can be caused in part by PCR amplification bias, where a subset of

fragments are preferentially amplified until they dominate the final library (Kanagawa 2003; Aird et al. 2011). These prior protocols utilized 18 cycles of amplification. We tested reducing this to 8, 10, 12, or 14 cycles and found that only 12 cycles were necessary to yield sufficient PCR product for sequencing; the reduction in the number of PCR cycles was expected to reduce PCR bias.

Another concern regarding previous sequencing results was an excess of long fragments (>700bps as determined by *in silico* digest), which do not provide sufficient reads to make confident genotype calls (< 5 reads per sample) and are therefore wasteful. We tested multiple methods of combatting this issue, including: reducing the PCR extension time, increasing the digestion length or enzyme concentration, increasing the selectivity of the primers, performing size selection on the libraries, or using a two-enzyme restriction digest.

We began by testing shorter extension times (15s/20s vs. 30s) to try and reduce the average fragment size of our sequencing libraries by preventing fragments with larger inserts from completing amplification. However, we did not see noticeable improvement in the final library composition at shorter extension times and determined the original length of 30 seconds was appropriate.

We also considered the possibility that the restriction enzyme digests might not be running to completion. To address this possibility, we increased the length of the digestion from 2 hours to 3 or 4 hours. We also tried increasing the number of units of PstI enzyme added, to ensure complete digest. Neither of these modifications impacted the final fragment length distribution of the library, indicating that the digest was reaching completion after 2 hours using the original concentration of PstI.

We also explored reducing the complexity of our library as a means of obtaining more reads at fewer sites. We accomplished this using the methods described by Sonah et al. 2013 (Sonah et al. 2013). This method involved adding an additional 1-2 nucleotides to the sequencing PCR primers (A or AG). The addition of these nucleotides increases the selectivity of the primers and reduces the number of amplifiable fragments, sacrificing sequencing breadth for read depth. However, this did not ameliorate the issue of reads being wasted on long fragments but did appear to increase the PCR bias (data not shown). Therefore, we chose to retain our original primer design.

Our previous GBS protocol did not have an explicit library fragment size selection step. The final library was purified using a MinElute PCR Purification Kit (QIAGEN Inc., Hilden, Germany), which isolates PCR products 70bp-4kb in length, leaving a wide range of fragment sizes in the final library, under the assumption that only shorter fragments would bridge amplify on the flow cell. This method was imprecise and had low reproducibility, negatively impacting our ability obtain reads at consistent sites across libraries. Rather than attempt size selection by gel extraction, we chose to utilize a Pippin Prep, which automates the elution of DNA libraries of desired fragment size ranges. By using this automated size selection, we reduced the proportion of the genome targeted for sequencing, and because restriction enzymes make the consistent cuts across samples, ensure the same fragments are sequenced in the majority of libraries. Since the clustering process involves a bridge amplification step that preferentially amplifies library fragments with shorter insert sizes (Illumina, Inc. 2014), we kept the size selection window narrow (250-400bps) to avoid introducing a bias in which fragments were sequenced.

To increase the proportion of the genome captured within the fragment size window, we pursued a double digest of the genome using a secondary enzyme with a more frequently occurring recognition sequence (Figure 1; Table 1). When used alone, *in silico* digest of the rn6 reference

genome by PstI (Figure 1; Table 1) showed that only ~0.5% of the genome would have fallen within a 150bp fragment size window selected on the Pippin Prep. Given the LD structure of other outbred rodent lines such as DO and CFW mice (Parker et al. 2016), we speculated this small fraction would not yield sufficient SNPs to tag the majority of variation in the genome. Additionally, we were concerned about potential biases in coverage, heterozygosity, and the minor allele frequency (**MAF**) spectrum that may be introduced by incomplete capture of the genome (Flanagan and Jones 2018). BfaI, MluCI, and NlaIII were chosen for further testing due to their compatibility with PstI digestion reagents and temperatures, sticky ends, and the proportion of the genome falling in the size selection window. We ruled out BfaI because it only had a 2bp overhang after cleavage, which led to a high concentration of adapter dimer in the sequencing libraries. NlaIII was chosen because it contained the greatest portion of the genome in the size selection window.

In our previous GBS protocol, all fragments were cut on both ends by PstI. By using a substantially lower concentration of the barcoded PstI adapter than the common PstI adapter, we ensured the barcoded adapter would be the limiting reagent and the majority of fragments with an annealed barcoded adapter would have a common adapter on the other end. This is crucial, as having one of each of the adapters is required for proper amplification of the fragments on the flow cell. However, when using both PstI and NlaIII, the library is predominantly composed of fragments cut on both sides by NlaIII, which will amplify during PCR with a common adapter, but not on the flow cell. Therefore, we employed a Y-adapter (Poland et al. 2012) to control the direction of the first round of PCR and prevent two-sided NlaIII fragments from dominating the final sequencing library (File S2).

We tested numerous quantities of PstI and NlaIII adapters in an attempt minimize the amount used and avoid adapter dimers in the final libraries. For the barcoded PstI adapters, we tested 120pmol, 40pmol, 20pmol, 4pmol, 3pmol, 1.5pmol, 0.6pmol, and 0.2pmol and for the NlaIII Y-adapter, 16pmol, 8pmol, 4pmol, 2pmol, 1pmol, and 0.5pmol. We found that 0.2pmol of PstI adapter and 4pmol of NlaIII Y-adapter yielded sufficient library and avoided adapter dimers.

We sequenced a trial flow cell with 8 pooled ddGBS libraries of 12 SD rat samples each (96 total) on a HiSeq 2500 (Illumina, San Diego, CA) with 125bp reads and v3 chemistry, obtaining an average of 15.3 million reads per sample. Given the NlaIII *in silico* digest results suggested we were capturing ~3.4% of the genome and that we were using 125bp reads, this corresponded to approximately 20x coverage of captured sites. We subsequently increased the number of samples to 48 per library for the HS rats because we hypothesized 5x would be sufficient coverage per sample when utilizing imputation to a reference panel. We also discovered that a portion of the reads contained sequence fragments of the NlaIII adapter sequence, indicating there were fragments with insert sizes smaller than 125bps in the final library. To avoid this, we increased the fragment size range to 300-450bps (Table 1), which corresponds to a 175-325bp insert size once the adapters and primers are accounted for. Due to the high concentrations of our libraries after pooling, the library size distribution obtained from the Pippin Prep was uniformly shifted towards higher fragment lengths (Figure S3).

The final ddGBS protocol can be found in File S1 and the necessary primer and adapter sequences in File S2. This protocol was used for the sequencing of all HS rats included in the following computational optimization steps.

Demultiplexing

The number of base pairs of sequencing data retained after demultiplexing was fairly consistent across demultiplexing software (Table S1). We ultimately decided to use FASTX Barcode Splitter because it yielded the greatest number of reads after quality/adapter trimming and had faster run times, though this may be predominantly attributable to outputting uncompressed FASTQ files. An average of 330 million 100bp reads were obtained per library, resulting in ~7 million reads per sample. Figure S4 shows the distribution of reads counts for all samples after demultiplexing, but prior to sample filtering based on read count.

Adapter and quality trimming

Read quality was substantially elevated after trimming the barcode and adapter sequences and low-quality base pairs at the ends of reads (Figure S5). Overall read counts were only marginally reduced by quality trimming (Table S1). We observed that the number of called variant sites and the genotyping rate were both greater when using reads initially processed by Cutadapt (Martin, 2011) than reads processed by the FASTX_Toolkit (Table S2). Importantly, a large portion of the additional identified variants were known variant sites from the 42 inbred strains reference set (Figure S6), indicating the elevated call rate was at least in part due to capturing more true variant sites. We viewed this as sufficient support for proceeding with Cutadapt for quality trimming.

Read alignment quality

The number of called variants and genotype call rates were identical at read mapping quality (mapQ) thresholds of either 20 or 30 (Table S3) within ANGSD. As the ANGSD mapQ threshold was raised to 45, there was a small reduction in the number of called variants, and then much greater losses at thresholds of 60 or 90. Fortunately, genotype concordance rates at both low and

high mapQ thresholds were stable, despite the putatively higher quality of the alignments (data not shown). This permitted us to select a lower mapQ threshold (mapQ = 20), maximizing the number of variants called without sacrificing genotype quality.

Variant calling

Neither GATK's UnifiedGenotyper nor HaplotypeCaller (McKenna et al. 2010; DePristo et al. 2011) called an adequate number of SNPs for fine-mapping in the HS. Panel A of Figure 3 shows that the combination of HaplotypeCaller and Beagle had lower rates of genotype concordance with array data than calls made by ANGSD and Beagle. We tried several adjustments to the GATK default thresholds for variant quality, heterozygosity, graph pruning, dangling branch length, and number of reads sharing an alignment start to declare an active region; however, none of these changes significantly improved the results (data not shown). As shown in Panel B of Figure 3, ANGSD/Beagle yielded a substantially greater number of SNPs at all genotyping error rate thresholds. This observation held when variants were limited only to biallelic sites and SNPs with an MAF > 0.05.

Figure 3. Genotype discordance rates between array data and variants called by GATK or ANGSD.

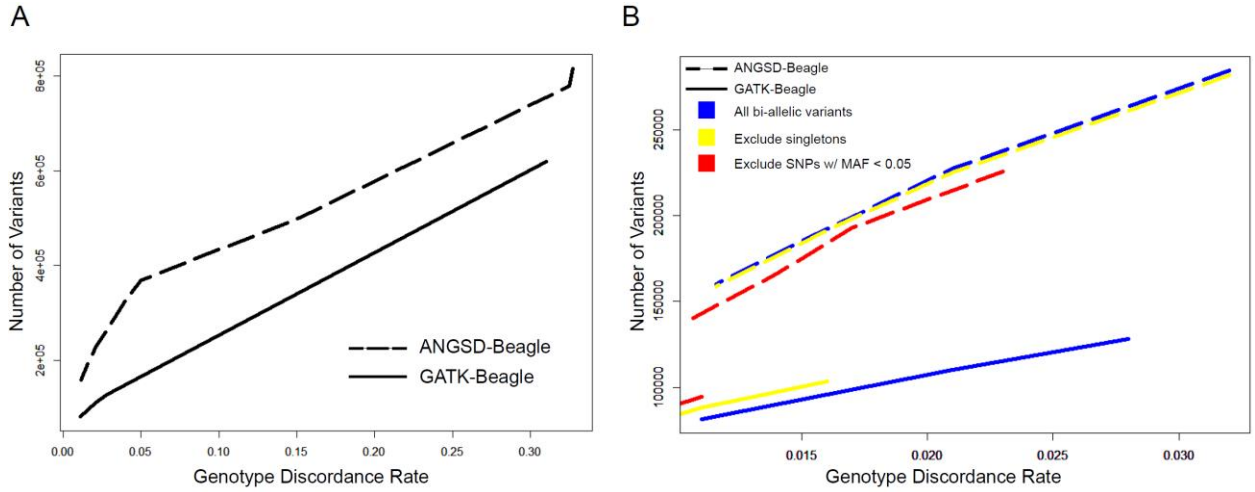

The two panels compare the number variants called by combination of ANGSD and Beagle or GATK HaplotypeCaller and Beagle at various thresholds of genotype discordance with array data. Calls were made using the 96 HS rats with array data. (A) The x-axis represents the genotype discordance rate thresholds and the y-axis is the number of variants that surpass that threshold for each genotype calling method. (B) Additional filters were applied to the original SNP sets and the plot zooms in on a smaller range of acceptable discordance rates. Blue lines represent the unfiltered SNP set. Yellow lines have been filtered for singletons. Red lines have further excluded SNPs with an MAF < 0.05. Each line contains the same number of points.

ANGSD supports four different models for estimating genotype likelihoods: SAMtools, GATK, SOAPsnp and SYK. We compared the methods to determine which produced the most SNPs with the lowest error rates. The SOAPsnp model demonstrated an advantage in genotype accuracy and number of variants called post-imputation with Beagle (Figure S7). However, SOAPsnp requires considerably more computational resources, outweighing its marginal benefits when applied to a large sample set (>2,000). The GATK model showed a greater number of variants for more lenient discordance rate threshold, but as stringency increased, the number of variants converged across the remaining 3 models. We proceeded with the SAMtools model for

genotype likelihood estimation due to its previous support in the GBS literature (Torkamaneh et al. 2017), accepting a nominal decrease in highly concordant variants for a large gain in efficiency.

Imputation to reference panel

Imputation is use in two ways in our protocol. As described above, we use imputation to assign missing genotypes at SNPs called in some but not all individuals. In addition, we use imputation in this section to call genotypes at site where GBS did not provide a call for any individuals. Thus, our second application (described here) is similar to the human genetics application in which imputation using 1000 Genomes increases the number of SNPs beyond those included on a given microarray platform.

Before starting this imputation step, we observed an inflated transition/transversion ratio (Table S4) in our ANGSD/Beagle SNPs. This issue was ameliorated when filtered the SNP set for only "known" variants that were previously identified in either the 42 inbred strains (Hermsen et al. 2015) or the 8 deep-sequenced HS founders (Ramdas et al. 2018). For imputation, we therefore only provided IMPUTE2 with previously identified variant sites from our ANGSD/Beagle output. Prior to running IMPUTE2, we also filtered the variants for biallelic sites with a genotype call in more than one individual. Using pedigree data for the HS rats, we further removed sites and samples showing uncharacteristically high levels of Mendelization errors. Lastly, we removed any samples where the sex chromosome read ratio was contrary to their reported sex (Figure S1).

To determine which reference set to use for imputation, we tested six different possible combinations of available reference data (Table 2). The most accurate imputation was observed for the reference set containing only the 8 deep-sequenced HS founder strains from UMich (Ramdas et al. 2018); however, imputation to this set had the lowest genotyping rate of all panels.

In contrast, using the 42 rat inbred strains displayed a balance of high accuracy and low missingness, leading us to choose this as our reference set. To better understand the role of the 8 founder strains, who were part of the 42 strains reference panel, we created a reference panel that included only the 34 non-HS founder strains. As expected, discordance rates were much higher when only considering non-founders. However, genotyping rates were greater for the 34 than the 8 founders, suggesting a combination of the two was the optimal set.

Table 2. Imputation accuracy based on different variant reference panels for IMPUTE2.

The table includes six different possible reference panels for imputation. The 42 inbred strains, 34 non-founder inbred strains, and 8 HS founders from the 42 inbred strains all were derived from Hermsen et al. 2015 (Hermsen et al. 2015). The UMich 8 HS founders were obtained from Ramdas et al. 2018 (Ramdas et al. 2018). The final set of 8 HS founder was taken from Baud et al. 2013 (Rat Genome Sequencing and Mapping Consortium et al. 2013).

		Chr1	Chr2
42 inbred strains	**Discordance rate**	0.011	0.010
	# Variants	790,659	882,993
	Genotyping Rate	0.85	0.81
UMich 8 founders + 42 inbred strains	**Discordance rate**	0.007	0.011
	# Variants	864,670	898,621
	Genotyping Rate	0.63	0.64
All 34 non-founder inbred strains	**Discordance rate**	0.035	0.030
	# Variants	812,550	912,749
	Genotyping Rate	0.84	0.80
8 HS founders only from the 42 inbred strains	**Discordance rate**	0.012	0.011
	# Variants	805,424	902,061
	Genotyping Rate	0.57	0.53
UMich 8 HS founders only	**Discordance rate**	0.0059	0.008
	# Variants	865,514	898,621
	Genotyping Rate	0.42	0.41
Baud et. al 2013 8 HS founders only	**Discordance rate**	0.0095	0.0096
	# Variants	507,909	540,844
	Genotyping Rate	0.43	0.40

IMPUTE2 requires a genetic map. As described in the methods section, we considered four different genetic maps, two that were empirically derived and two that were linear extrapolations based on the physical map. All genetic map performed similarly (Table S5). Surprisingly, the linear genetic maps performed just as well as the HS-specific map (Littrell et al. 2018). Thus, for simplicity, we chose to use the chromosome-specific values initially published by Jensen-Seaman (Jensen-Seaman 2004).

Pre-phasing with VCFtools and IMPUTE2 performed similarly, therefore we used IMPUTE2. SHAPEIT was not used because it showed a higher rate of genotype discordance compared to VCFtools and IMPUTE2 (data not shown).

To obtain our final set of ~3.7 million variants, a final round of variant filtering was performed after imputation to the 42 strain reference panel. We removed SNPs with MAF < 0.005, a post-imputation genotyping rate < 90%, and SNPs that violated HWE with $p<1x10^{-10}$.

DISCUSSION

The use of microarrays and WGS for genotyping large samples in model organisms remains cost-prohibitive. There is therefore an urgent and wide-spread need for a high-performance and economical methods of obtaining genome-wide genotype data. While reduced-representation approaches have been utilized in numerous species of plants and animals, including rodents (Peterson et al. 2012; Fitzpatrick et al. 2013; Parker et al. 2016; Gonzales et al. 2017; Zhou et al. 2018), there has yet to be a published protocol optimized specifically for rats. Prior to sequencing thousands of HS samples with GBS for our mapping efforts, we wanted to ensure we were capturing the greatest possible number of high-quality variants at the lowest possible cost. The

protocol we present here is the culmination of careful testing and optimization of each step of the GBS protocol for rats. We have now applied the approach to 4,973 HS rats, as well as 4,608 Sprague Dawley rats (Gileta et al. 2018).

Our previous GBS protocol (Parker *et al*, 2016), which was designed for use with CFW mice, was unsuitable for our current genotyping efforts in HS rats, due to the much higher levels of genetic diversity in the HS population. There are multiple reasons we chose to develop our own computational pipeline for GBS rather than using existing workflows. Foremost, the prominent GBS analysis pipelines were developed and optimized for use in crop species (Sonah et al. 2013; Catchen et al. 2013; Glaubitz et al. 2014; Torkamaneh et al. 2017; Wickland et al. 2017), which are polyploid and have differing levels of variation and LD than outbred rodent populations. Additionally, there were elements of each pipeline that did not meet our needs or lacked customizability. For instance, TASSEL-GBS v2 (Glaubitz et al. 2014) trims all reads to 92 base pairs; however, other projects underway in our lab utilized up to 125bp reads, leading to a ~20% reduction in data. TASSEL-GBS also ignores read base quality scores, which are informative in probabilistic frameworks for estimating uncertainty in alignments and variant calls (H. Li, Ruan, and Durbin 2008; DePristo et al. 2011; Nielsen et al. 2011), and uses a naïve binomial likelihood ratio method for calling SNPs. Stacks has previously shown poor demultiplexing (Herten et al. 2015; Torkamaneh et al. 2017) and does not make use of the reference genome for priors when calling SNPs (Catchen et al. 2013). Fast-GBS relies on Platypus for variant calling (WGS500 Consortium et al. 2014; Torkamaneh et al. 2017), which employs a Bayesian method of constructing candidate haplotypes that works poorly with low-pass sequencing data and does not scale well (Z. Li, Wang, and Wang 2018). Lastly, none of these pipelines included an imputation step, which is crucial for filling in missing genotypes in GBS data and can provide millions of

additional SNPs given an appropriate composite reference panel (B. Howie, Marchini, and Stephens 2011; G.-H. Huang and Tseng 2014).

Though we have not explicitly tested each alternate GBS pipeline for the purposes of this publication, this has been recently done by Wickland et al. (Wickland et al. 2017). Their pipeline GB-eaSy, which ours most closely resembles, was found to be superior by a number of metrics to Stacks, TASSEL-GBS, IGST, and Fast-GBS. Similar to GB-eaSy, our pipeline utilizes a double-digest GBS protocol, aligns reads to the reference genome with *bwa-mem*, and uses the SAMtools genotype likelihood model for calling SNPs (H. Li 2011). The combination of bwa-mem and SAMtools algorithm was independently shown to have the best performance for calling SNPs from Illumina data (Hwang et al. 2015), further supporting our choice of these programs for read alignment and variant calling. Additionally, using the ANGSD wrapper provided us with the ability to convert the posterior genotype probabilities into genotype dosages for mapping studies (Korneliussen, Albrechtsen, and Nielsen 2014).

A minor difference between GB-eaSy and our pipeline is the use of Cutadapt (Martin 2011) rather than GBSX (Herten et al. 2015) for demultiplexing, though both performed equally well (Table S1). The primary improvement is our extension of the pipeline with the implementation of effective internal and reference-based imputation steps using the 42 inbred rat genomes (Hermsen et al. 2015) and 8 deep-sequenced HS founders from UMich (Ramdas et al. 2018). There are two stages of imputation in our pipeline: the first one is accomplished by Beagle, and aims to fill in missing genotypes at called variants using information from other samples; this raises the genotype call rate to 100% but may also introduce errors if there is low confidence in the existing genotype calls, emphasizing the need for careful filtering steps. The second stage of imputation made use of IMPTUE2 and an external reference panels of variants called from WGS data on the 8 inbred HS

founders, as well as 34 additional inbred rat strains. We decided to include the 34 additional strains because of the elevated genotyping rate we observed upon their inclusion in the IMPUTE2 reference panel. We attribute this to the presence of haplotypes that exist in both the 8 the HS founder strains and a subset of the 34 additional strains in this panel.

In summary, we have adapted a GBS protocol and genotyping and imputation pipeline to obtain dense genotypes on genome-wide markers in highly-multiplexed HS rats. After quality filtering on the level of SNP and sample, over 3.7 million were called with a concordance rate of 99%. The ddGBS protocol and bioinformatic methods used to produce this data are publicly available, easy to handle, and cost-effective. The presented workflow could be feasibly followed with marginal modifications for application in other species.

ACKNOWLEDGEMENTS:

This work was supported by P50 DA037844, R21 DA036672, T32 GM07197, and F31 DA039638.

LITERATURE CITED

Aird, Daniel, Michael G Ross, Wei-Sheng Chen, Maxwell Danielsson, Timothy Fennell, Carsten Russ, David B Jaffe, Chad Nusbaum, and Andreas Gnirke. 2011. "Analyzing and Minimizing PCR Amplification Bias in Illumina Sequencing Libraries." *Genome Biology* 12 (2): R18. https://doi.org/10.1186/gb-2011-12-2-r18.

Andrews, Simon. 2017. *FastQC* (version 0.11.6). http://www.bioinformatics.babraham.ac.uk/projects/fastqc/.

Baird, Nathan A., Paul D. Etter, Tressa S. Atwood, Mark C. Currey, Anthony L. Shiver, Zachary A. Lewis, Eric U. Selker, William A. Cresko, and Eric A. Johnson. 2008. "Rapid SNP Discovery and Genetic Mapping Using Sequenced RAD Markers." Edited by Justin C. Fay. *PLoS ONE* 3 (10): e3376. https://doi.org/10.1371/journal.pone.0003376.

Browning, Brian L., and Sharon R. Browning. 2009. "A Unified Approach to Genotype Imputation and Haplotype-Phase Inference for Large Data Sets of Trios and Unrelated Individuals." *The American Journal of Human Genetics* 84 (2): 210–23. https://doi.org/10.1016/j.ajhg.2009.01.005.

Browning, Brian L., and Sharon R. Browning. 2016. "Genotype Imputation with Millions of Reference Samples." *The American Journal of Human Genetics* 98 (1): 116–26. https://doi.org/10.1016/j.ajhg.2015.11.020.

Catchen, Julian, Paul A. Hohenlohe, Susan Bassham, Angel Amores, and William A. Cresko. 2013. "Stacks: An Analysis Tool Set for Population Genomics." *Molecular Ecology* 22 (11): 3124–40. https://doi.org/10.1111/mec.12354.

Chen, Qiang, Yufang Ma, Yumei Yang, Zhenliang Chen, Rongrong Liao, Xiaoxian Xie, Zhen Wang, et al. 2013. "Genotyping by Genome Reducing and Sequencing for Outbred Animals." Edited by Shuhong Zhao. *PLoS ONE* 8 (7): e67500. https://doi.org/10.1371/journal.pone.0067500.

Chitre, Apurva S, Oksana Polesskaya, Katie Holl, Jianjun Gao, Riyan Cheng, Angel Martinez, Tony George, et al. 2018. "Genome Wide Association Study of Body Weight, Body Mass Index, Adiposity, and Fasting Glucose in 3,173 Outbred Rats," September. https://doi.org/10.1101/422428.

Danecek, P., A. Auton, G. Abecasis, C. A. Albers, E. Banks, M. A. DePristo, R. E. Handsaker, et al. 2011. "The Variant Call Format and VCFtools." *Bioinformatics* 27 (15): 2156–58. https://doi.org/10.1093/bioinformatics/btr330.

Davey, John W., Paul A. Hohenlohe, Paul D. Etter, Jason Q. Boone, Julian M. Catchen, and Mark L. Blaxter. 2011. "Genome-Wide Genetic Marker Discovery and Genotyping Using next-Generation Sequencing." *Nature Reviews Genetics* 12 (7): 499–510. https://doi.org/10.1038/nrg3012.

De Donato, Marcos, Sunday O. Peters, Sharon E. Mitchell, Tanveer Hussain, and Ikhide G. Imumorin. 2013. "Genotyping-by-Sequencing (GBS): A Novel, Efficient and Cost-Effective Genotyping Method for Cattle Using Next-Generation Sequencing." Edited by James C. Nelson. *PLoS ONE* 8 (5): e62137. https://doi.org/10.1371/journal.pone.0062137.

Delaneau, Olivier, Jonathan Marchini, and Jean-François Zagury. 2011. "A Linear Complexity Phasing Method for Thousands of Genomes." *Nature Methods* 9 (December): 179.

DePristo, Mark A, Eric Banks, Ryan Poplin, Kiran V Garimella, Jared R Maguire, Christopher Hartl, Anthony A Philippakis, et al. 2011. "A Framework for Variation Discovery and Genotyping Using Next-Generation DNA Sequencing Data." *Nature Genetics* 43 (5): 491–98. https://doi.org/10.1038/ng.806.

Durvasula, Arun, Paul J Hoffman, Tyler V Kent, Chaochih Liu, Thomas J Y Kono, Peter L Morrell, and Jeffrey Ross-Ibarra. n.d. "ANGSD-Wrapper: Utilities for Analyzing next Generation Sequencing Data." Accessed September 5, 2018. https://doi.org/10.7287/peerj.preprints.1472v2.

Elshire, Robert J., Jeffrey C. Glaubitz, Qi Sun, Jesse A. Poland, Ken Kawamoto, Edward S. Buckler, and Sharon E. Mitchell. 2011. "A Robust, Simple Genotyping-by-Sequencing (GBS) Approach for High Diversity Species." Edited by Laszlo Orban. *PLoS ONE* 6 (5): e19379. https://doi.org/10.1371/journal.pone.0019379.

Fitzpatrick, Christopher J., Shyam Gopalakrishnan, Elizabeth S. Cogan, Lindsay M. Yager, Paul J. Meyer, Vedran Lovic, Benjamin T. Saunders, et al. 2013. "Variation in the Form of Pavlovian Conditioned Approach Behavior among Outbred Male Sprague-Dawley Rats from Different Vendors and Colonies: Sign-Tracking vs. Goal-Tracking." Edited by Patrizia Campolongo. *PLoS ONE* 8 (10): e75042. https://doi.org/10.1371/journal.pone.0075042.

Flanagan, Sarah P., and Adam G. Jones. 2018. "Substantial Differences in Bias between Single-Digest and Double-Digest RAD-Seq Libraries: A Case Study." *Molecular Ecology Resources* 18 (2): 264–80. https://doi.org/10.1111/1755-0998.12734.

Fu, Yong-Bi, and Mo-Hua Yang. 2017. "Genotyping-by-Sequencing and Its Application to Oat Genomic Research." In *Oat*, edited by Sebastian Gasparis, 1536:169–87. New York, NY: Springer New York. https://doi.org/10.1007/978-1-4939-6682-0_13.

Furuta, Tomoyuki, Motoyuki Ashikari, Kshirod K. Jena, Kazuyuki Doi, and Stefan Reuscher. 2017. "Adapting Genotyping-by-Sequencing for Rice F2 Populations." *G3: Genes|Genomes|Genetics* 7 (3): 881–93. https://doi.org/10.1534/g3.116.038190.

Gileta, Alexander F., Christopher J. Fitzpatrick, Apurva S. Chitre, Celine L. St. Pierre, Elizabeth V. Joyce, Rachael J. Maguire, Africa M. McLeod, et al. 2018. "Genetic Characterization of Outbred Sprague Dawley Rats and Utility for Genome-Wide Association Studies," September. https://doi.org/10.1101/412924.

Glaubitz, Jeffrey C., Terry M. Casstevens, Fei Lu, James Harriman, Robert J. Elshire, Qi Sun, and Edward S. Buckler. 2014. "TASSEL-GBS: A High Capacity Genotyping by Sequencing Analysis Pipeline." Edited by Nicholas A. Tinker. *PLoS ONE* 9 (2): e90346. https://doi.org/10.1371/journal.pone.0090346.

Gonzales, Natalia M., Jungkyun Seo, Ana Isabel Hernandez-Cordero, Celine L. St. Pierre, Jennifer S. Gregory, Margaret G. Distler, Mark Abney, Stefan Canzar, Arimantas Lionikas, and Abraham A. Palmer. 2017. "Genome Wide Association Study of Behavioral, Physiological and Gene Expression Traits in a Multigenerational Mouse Intercross," December. https://doi.org/10.1101/230920.

———. 2018. "Genome Wide Association Analysis in a Mouse Advanced Intercross Line," September. https://doi.org/10.1101/230920.

Hannon Lab. 2010. *FASTX-Toolkit* (version 0.0.13). http://hannonlab.cshl.edu/fastx_toolkit/index.html.

He, Jiangfeng, Xiaoqing Zhao, AndrÃ© Laroche, Zhen-Xiang Lu, HongKui Liu, and Ziqin Li. 2014. "Genotyping-by-Sequencing (GBS), an Ultimate Marker-Assisted Selection (MAS) Tool to Accelerate Plant Breeding." *Frontiers in Plant Science* 5 (September). https://doi.org/10.3389/fpls.2014.00484.

Hermsen, Roel, Joep de Ligt, Wim Spee, Francis Blokzijl, Sebastian Schäfer, Eleonora Adami, Sander Boymans, et al. 2015. "Genomic Landscape of Rat Strain and Substrain Variation." *BMC Genomics* 16 (1). https://doi.org/10.1186/s12864-015-1594-1.

Herten, Koen, Matthew S Hestand, Joris R Vermeesch, and Jeroen KJ Van Houdt. 2015. "GBSX: A Toolkit for Experimental Design and Demultiplexing Genotyping by Sequencing Experiments." *BMC Bioinformatics* 16 (1). https://doi.org/10.1186/s12859-015-0514-3.

Howie, Bryan, Christian Fuchsberger, Matthew Stephens, Jonathan Marchini, and Gonçalo R Abecasis. 2012. "Fast and Accurate Genotype Imputation in Genome-Wide Association Studies through Pre-Phasing." *Nature Genetics* 44 (July): 955.

670 Howie, Bryan, Jonathan Marchini, and Matthew Stephens. 2011. “Genotype Imputation with Thousands
671 of Genomes.” *G3: Genes|Genomes|Genetics* 1 (6): 457–70.
672 https://doi.org/10.1534/g3.111.001198.
673 Howie, Bryan N., Peter Donnelly, and Jonathan Marchini. 2009. “A Flexible and Accurate Genotype
674 Imputation Method for the Next Generation of Genome-Wide Association Studies.” Edited by
675 Nicholas J. Schork. *PLoS Genetics* 5 (6): e1000529.
676 https://doi.org/10.1371/journal.pgen.1000529.
677 Huang, Guan-Hua, and Yi-Chi Tseng. 2014. “Genotype Imputation Accuracy with Different Reference
678 Panels in Admixed Populations.” *BMC Proceedings* 8 (Suppl 1): S64.
679 https://doi.org/10.1186/1753-6561-8-S1-S64.
680 Huang, X., Q. Feng, Q. Qian, Q. Zhao, L. Wang, A. Wang, J. Guan, et al. 2009. “High-Throughput
681 Genotyping by Whole-Genome Resequencing.” *Genome Research* 19 (6): 1068–76.
682 https://doi.org/10.1101/gr.089516.108.
683 Hwang, Sohyun, Eiru Kim, Insuk Lee, and Edward M. Marcotte. 2015. “Systematic Comparison of Variant
684 Calling Pipelines Using Gold Standard Personal Exome Variants.” *Scientific Reports* 5 (December):
685 17875.
686 Illumina, Inc. 2014. “Nextera(R) Library Validation and Cluster Density Optimization: Guidelines for
687 Generating High-Quality Data with Nextera Library Prepartion Kits.”
688 https://www.illumina.com/documents/products/technotes/technote_nextera_library_validatio
689 n.pdf.
690 Jensen-Seaman, M. I. 2004. “Comparative Recombination Rates in the Rat, Mouse, and Human
691 Genomes.” *Genome Research* 14 (4): 528–38. https://doi.org/10.1101/gr.1970304.
692 Johannesson, M., R. Lopez-Aumatell, P. Stridh, M. Diez, J. Tuncel, G. Blazquez, E. Martinez-Membrives,
693 et al. 2008. “A Resource for the Simultaneous High-Resolution Mapping of Multiple Quantitative
694 Trait Loci in Rats: The NIH Heterogeneous Stock.” *Genome Research* 19 (1): 150–58.
695 https://doi.org/10.1101/gr.081497.108.
696 Johnson, Jennifer L., Helena Wittgenstein, Sharon E. Mitchell, Katie E. Hyma, Svetlana V. Temnykh,
697 Anastasiya V. Kharlamova, Rimma G. Gulevich, et al. 2015. “Genotyping-By-Sequencing (GBS)
698 Detects Genetic Structure and Confirms Behavioral QTL in Tame and Aggressive Foxes (Vulpes
699 Vulpes).” Edited by William J. Murphy. *PLOS ONE* 10 (6): e0127013.
700 https://doi.org/10.1371/journal.pone.0127013.
701 Kanagawa, Takahiro. 2003. “Bias and Artifacts in Multitemplate Polymerase Chain Reactions (PCR).”
702 *Journal of Bioscience and Bioengineering* 96 (4): 317–23. https://doi.org/10.1016/S1389-
703 1723(03)90130-7.
704 Kent, W. J., C. W. Sugnet, T. S. Furey, K. M. Roskin, T. H. Pringle, A. M. Zahler, and a. D. Haussler. 2002.
705 “The Human Genome Browser at UCSC.” *Genome Research* 12 (6): 996–1006.
706 https://doi.org/10.1101/gr.229102.
707 Korneliussen, Thorfinn Sand, Anders Albrechtsen, and Rasmus Nielsen. 2014. “ANGSD: Analysis of Next
708 Generation Sequencing Data.” *BMC Bioinformatics* 15 (1). https://doi.org/10.1186/s12859-014-
709 0356-4.
710 Li, H. 2011. “A Statistical Framework for SNP Calling, Mutation Discovery, Association Mapping and
711 Population Genetical Parameter Estimation from Sequencing Data.” *Bioinformatics* 27 (21):
712 2987–93. https://doi.org/10.1093/bioinformatics/btr509.
713 Li, H., and R. Durbin. 2009. “Fast and Accurate Short Read Alignment with Burrows-Wheeler Transform.”
714 *Bioinformatics* 25 (14): 1754–60. https://doi.org/10.1093/bioinformatics/btp324.
715 Li, H., J. Ruan, and R. Durbin. 2008. “Mapping Short DNA Sequencing Reads and Calling Variants Using
716 Mapping Quality Scores.” *Genome Research* 18 (11): 1851–58.
717 https://doi.org/10.1101/gr.078212.108.

Li, Zhentang, Yi Wang, and Fei Wang. 2018. “A Study on Fast Calling Variants from Next-Generation Sequencing Data Using Decision Tree.” *BMC Bioinformatics* 19 (1). https://doi.org/10.1186/s12859-018-2147-9.

Littrell, John, Shirng-Wern Tsaih, Amelie Baud, Pasi Rastas, Leah Solberg-Woods, and Michael J. Flister. 2018. “A High-Resolution Genetic Map for the Laboratory Rat.” *G3: Genes|Genomes|Genetics*, May, g3.200187.2018. https://doi.org/10.1534/g3.118.200187.

Martin, Marcel. 2011. “Cutadapt Removes Adapter Sequences from High-Throughput Sequencing Reads.” *EMBnet.Journal* 17 (1): 10. https://doi.org/10.14806/ej.17.1.200.

McKenna, A., M. Hanna, E. Banks, A. Sivachenko, K. Cibulskis, A. Kernytsky, K. Garimella, et al. 2010. “The Genome Analysis Toolkit: A MapReduce Framework for Analyzing next-Generation DNA Sequencing Data.” *Genome Research* 20 (9): 1297–1303. https://doi.org/10.1101/gr.107524.110.

Miller, M. R., J. P. Dunham, A. Amores, W. A. Cresko, and E. A. Johnson. 2007. “Rapid and Cost-Effective Polymorphism Identification and Genotyping Using Restriction Site Associated DNA (RAD) Markers.” *Genome Research* 17 (2): 240–48. https://doi.org/10.1101/gr.5681207.

Nielsen, Rasmus, Joshua S. Paul, Anders Albrechtsen, and Yun S. Song. 2011. “Genotype and SNP Calling from Next-Generation Sequencing Data.” *Nature Reviews Genetics* 12 (6): 443–51. https://doi.org/10.1038/nrg2986.

Orsouw, Nathalie J. van, René C. J. Hogers, Antoine Janssen, Feyruz Yalcin, Sandor Snoeijers, Esther Verstege, Harrie Schneiders, et al. 2007. “Complexity Reduction of Polymorphic Sequences (CRoPS^{TM}): A Novel Approach for Large-Scale Polymorphism Discovery in Complex Genomes.” Edited by Ivan Baxter. *PLoS ONE* 2 (11): e1172. https://doi.org/10.1371/journal.pone.0001172.

Parker, Clarissa C, Shyam Gopalakrishnan, Peter Carbonetto, Natalia M Gonzales, Emily Leung, Yeonhee J Park, Emmanuel Aryee, et al. 2016. “Genome-Wide Association Study of Behavioral, Physiological and Gene Expression Traits in Outbred CFW Mice.” *Nature Genetics* 48 (8): 919–26. https://doi.org/10.1038/ng.3609.

Pértille, Fábio, Carlos Guerrero-Bosagna, Vinicius Henrique da Silva, Clarissa Boschiero, José de Ribamar da Silva Nunes, Mônica Corrêa Ledur, Per Jensen, and Luiz Lehmann Coutinho. 2016. “High-Throughput and Cost-Effective Chicken Genotyping Using Next-Generation Sequencing.” *Scientific Reports* 6 (May): 26929.

Peterson, Brant K., Jesse N. Weber, Emily H. Kay, Heidi S. Fisher, and Hopi E. Hoekstra. 2012. “Double Digest RADseq: An Inexpensive Method for De Novo SNP Discovery and Genotyping in Model and Non-Model Species.” Edited by Ludovic Orlando. *PLoS ONE* 7 (5): e37135. https://doi.org/10.1371/journal.pone.0037135.

Poland, Jesse A., Patrick J. Brown, Mark E. Sorrells, and Jean-Luc Jannink. 2012. “Development of High-Density Genetic Maps for Barley and Wheat Using a Novel Two-Enzyme Genotyping-by-Sequencing Approach.” Edited by Tongming Yin. *PLoS ONE* 7 (2): e32253. https://doi.org/10.1371/journal.pone.0032253.

Purcell, Shaun. 2014. *PLINK/SEQ: A Library for the Analysis of Genetic Variation Data* (version v0.10). http://atgu.mgh.harvard.edu/plinkseq/index.shtml.

Ramdas, Shweta, Ayse Bilge Ozel, Katie Holl, Myrna Mandel, Leah Solberg Woods, and Jun Z Li. 2018. “Extended Regions of Suspected Mis-Assembly in the Rat Reference Genome,” September. https://doi.org/10.1101/332932.

Rat Genome Sequencing and Mapping Consortium, Amelie Baud, Roel Hermsen, Victor Guryev, Pernilla Stridh, Delyth Graham, Martin W McBride, et al. 2013. “Combined Sequence-Based and Genetic Mapping Analysis of Complex Traits in Outbred Rats.” *Nature Genetics* 45 (7): 767–75. https://doi.org/10.1038/ng.2644.

765 Rice, Peter, Ian Longden, and Alan Bleasby. 2000. "EMBOSS: The European Molecular Biology Open
766 Software Suite." *Trends in Genetics* 16 (6): 276–77. https://doi.org/10.1016/S0168-
767 9525(00)02024-2.
768 Roberts, R. J., and D. Macelis. 1999. "REBASE--Restriction Enzymes and Methylases." *Nucleic Acids*
769 *Research* 27 (1): 312–13. https://doi.org/10.1093/nar/27.1.312.
770 Scheben, Armin, Jacqueline Batley, and David Edwards. 2017. "Genotyping-by-Sequencing Approaches
771 to Characterize Crop Genomes: Choosing the Right Tool for the Right Application." *Plant*
772 *Biotechnology Journal* 15 (2): 149–61. https://doi.org/10.1111/pbi.12645.
773 Sonah, Humira, Maxime Bastien, Elmer Iquira, Aurélie Tardivel, Gaétan Légaré, Brian Boyle, Éric
774 Normandeau, et al. 2013. "An Improved Genotyping by Sequencing (GBS) Approach Offering
775 Increased Versatility and Efficiency of SNP Discovery and Genotyping." Edited by Zhanjiang Liu.
776 *PLoS ONE* 8 (1): e54603. https://doi.org/10.1371/journal.pone.0054603.
777 Steen, R. G., A. E. Kwitek-Black, C. Glenn, J. Gullings-Handley, W. Van Etten, O. S. Atkinson, D. Appel, et
778 al. 1999. "A High-Density Integrated Genetic Linkage and Radiation Hybrid Map of the
779 Laboratory Rat." *Genome Research* 9 (6): AP1-8, insert.
780 Sun, Xiaowen, Dongyuan Liu, Xiaofeng Zhang, Wenbin Li, Hui Liu, Weiguo Hong, Chuanbei Jiang, et al.
781 2013. "SLAF-Seq: An Efficient Method of Large-Scale De Novo SNP Discovery and Genotyping
782 Using High-Throughput Sequencing." Edited by Jan Aerts. *PLoS ONE* 8 (3): e58700.
783 https://doi.org/10.1371/journal.pone.0058700.
784 Torkamaneh, Davoud, Jérôme Laroche, Maxime Bastien, Amina Abed, and François Belzile. 2017. "Fast-
785 GBS: A New Pipeline for the Efficient and Highly Accurate Calling of SNPs from Genotyping-by-
786 Sequencing Data." *BMC Bioinformatics* 18 (1). https://doi.org/10.1186/s12859-016-1431-9.
787 Van Tassell, Curtis P, Timothy P L Smith, Lakshmi K Matukumalli, Jeremy F Taylor, Robert D Schnabel,
788 Cynthia Taylor Lawley, Christian D Haudenschild, Stephen S Moore, Wesley C Warren, and Tad S
789 Sonstegard. 2008. "SNP Discovery and Allele Frequency Estimation by Deep Sequencing of
790 Reduced Representation Libraries." *Nature Methods* 5 (3): 247–52.
791 https://doi.org/10.1038/nmeth.1185.
792 Wang, Yuzhe, Xuemin Cao, Yiqiang Zhao, Jing Fei, Xiaoxiang Hu, and Ning Li. 2017. "Optimized Double-
793 Digest Genotyping by Sequencing (DdGBS) Method with High-Density SNP Markers and High
794 Genotyping Accuracy for Chickens." Edited by Peng Xu. *PLOS ONE* 12 (6): e0179073.
795 https://doi.org/10.1371/journal.pone.0179073.
796 WGS500 Consortium, Andy Rimmer, Hang Phan, Iain Mathieson, Zamin Iqbal, Stephen R F Twigg,
797 Andrew O M Wilkie, Gil McVean, and Gerton Lunter. 2014. "Integrating Mapping-, Assembly-
798 and Haplotype-Based Approaches for Calling Variants in Clinical Sequencing Applications."
799 *Nature Genetics* 46 (8): 912–18. https://doi.org/10.1038/ng.3036.
800 Wickland, Daniel P., Gopal Battu, Karen A. Hudson, Brian W. Diers, and Matthew E. Hudson. 2017. "A
801 Comparison of Genotyping-by-Sequencing Analysis Methods on Low-Coverage Crop Datasets
802 Shows Advantages of a New Workflow, GB-EaSy." *BMC Bioinformatics* 18 (1).
803 https://doi.org/10.1186/s12859-017-2000-6.
804 Woods, Leah C. Solberg, and Richard Mott. 2017. "Heterogeneous Stock Populations for Analysis of
805 Complex Traits." In *Systems Genetics*, edited by Klaus Schughart and Robert W. Williams,
806 1488:31–44. New York, NY: Springer New York. https://doi.org/10.1007/978-1-4939-6427-7_2.
807 Zhou, Xinzhu, Celine L. St. Pierre, Natalia M. Gonzales, Riyan Cheng, Apurva S. Chitre, Greta Sokoloff, and
808 Abraham A. Palmer. 2018. "Genome-Wide Association Study, Replication, and Mega-Analysis
809 Using a Dense Marker Panel in a Multi-Generational Mouse Advanced Intercross Line," August.
810 https://doi.org/10.1101/387613.
811

Figure S1. Ratio of reads on X-chromosome to total sequencing reads.

The color of the points indicates the pedigree-recorded sex of the samples. Females are expected to have approximately twice as many reads for the X-chromosome. Samples that did not cluster with their pedigree-recorded sex were removed from the study for possible sample mix-up.

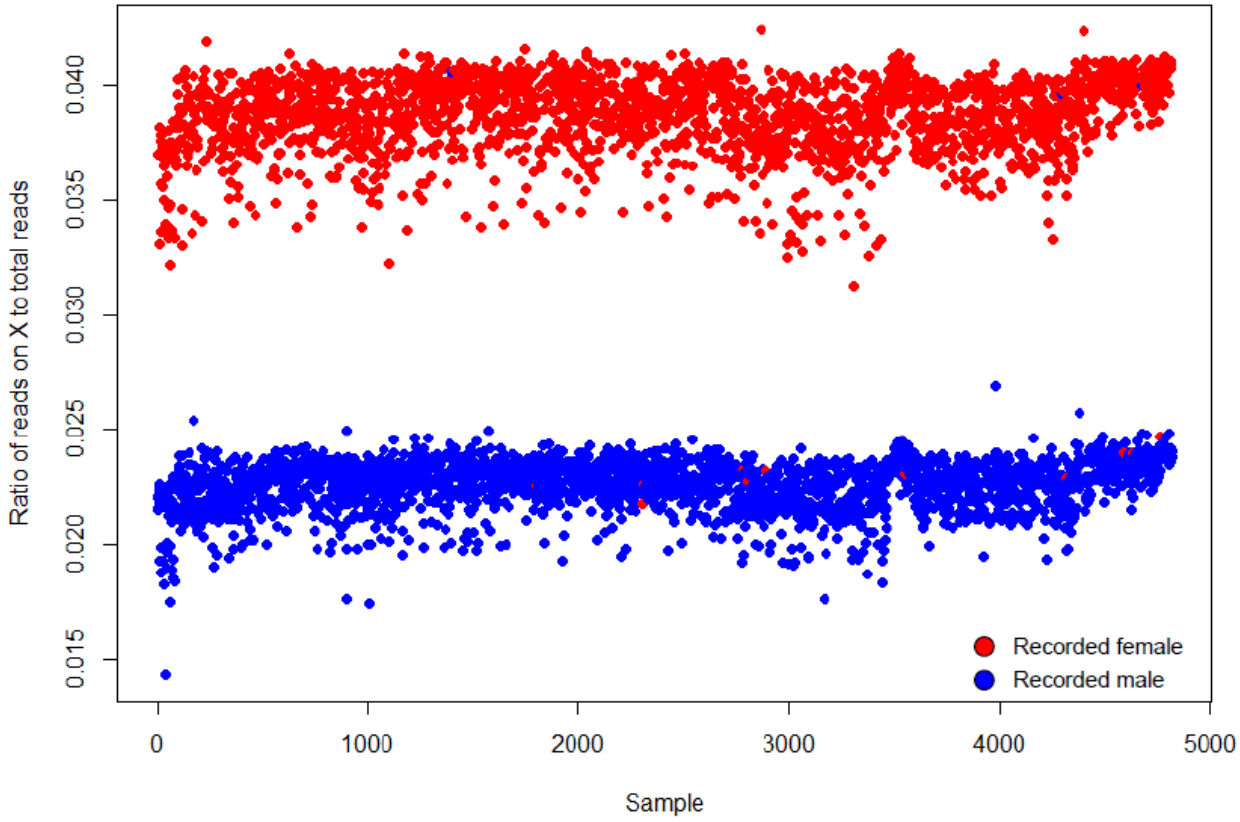

Figure S2. Data preparation workflow for imputation with IMPUTE2.

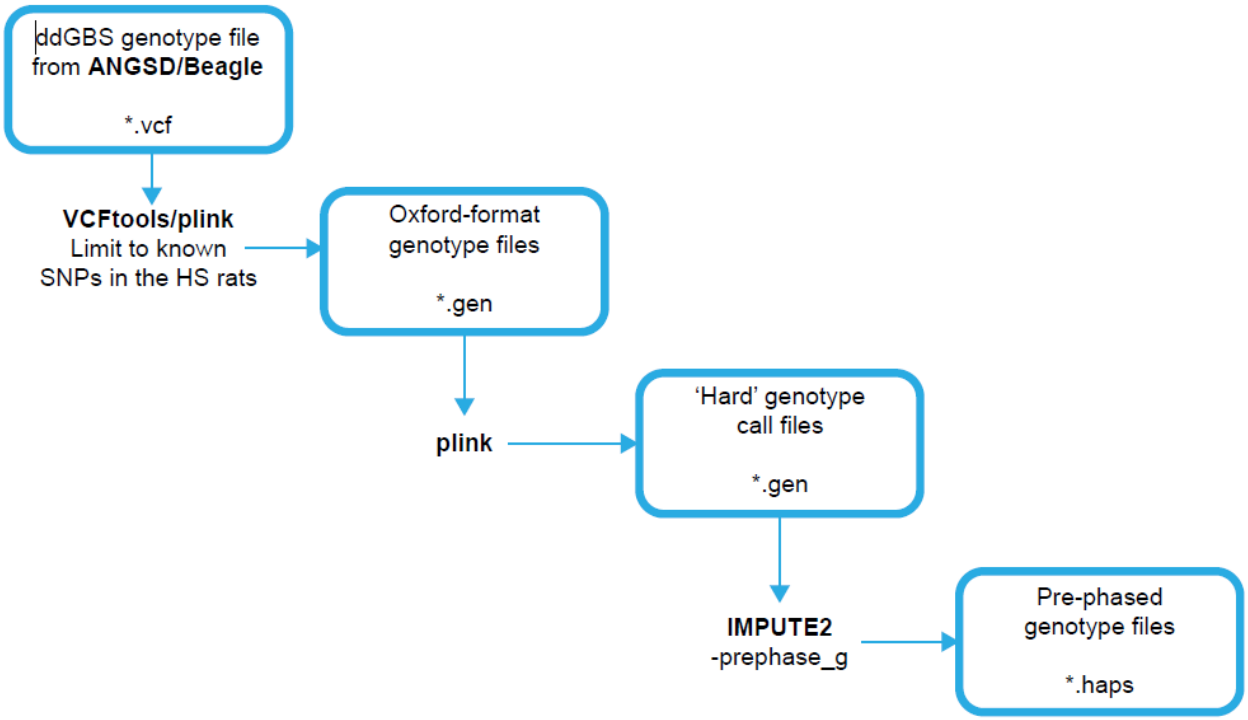

Figure S3. Programmed vs. empirical Pippin Prep fragment size range.

This plot comes from the Bioanalyzer output for a pooled HS library. The x-axis shows the library fragment sizes in base pairs, and the y-axis is in fluorescent units, which represent the quantity of the fragments on the gel chip. There is approximately a 50-75bp shift in the empirical library distribution compared to expectation due to the high quantity of fragments loaded into the Pippin Prep gel cassette.

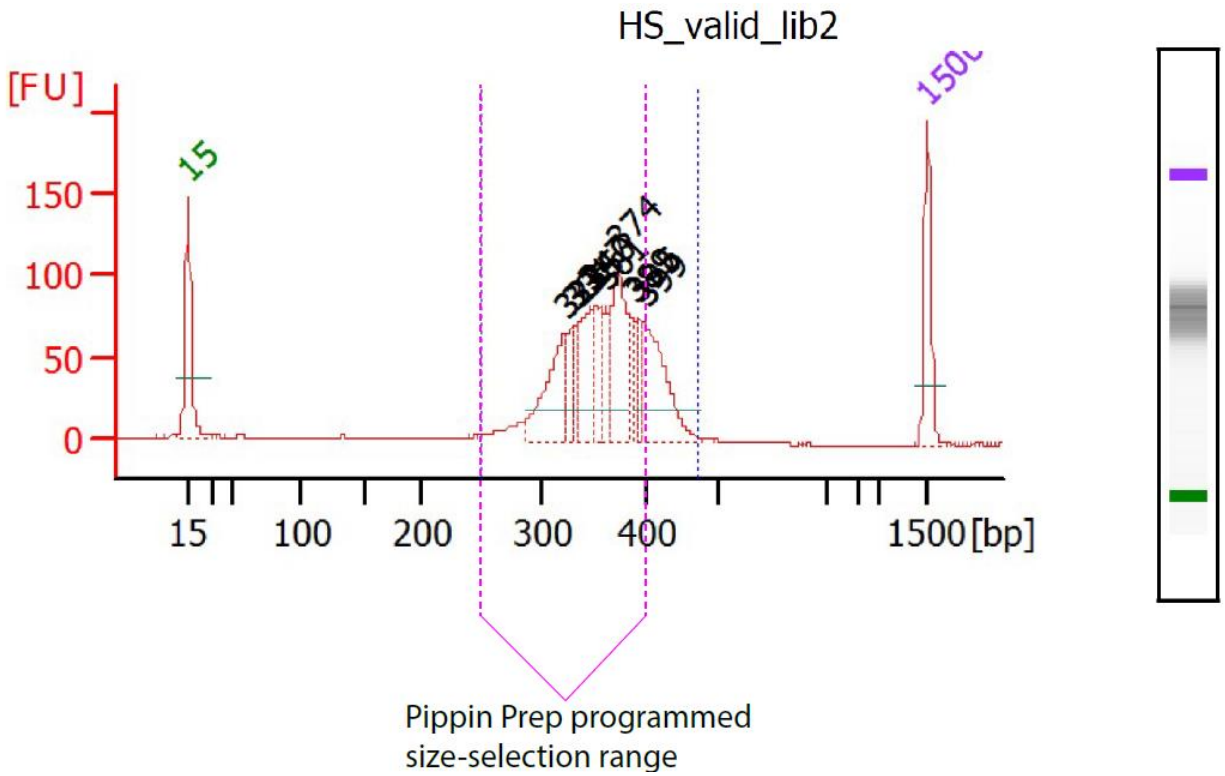

Figure S4. Raw read counts grouped by shipment batch.

Raw read counts are on a per-sample basis after demultiplexing FASTQ files with FASTX Barcode Splitter.

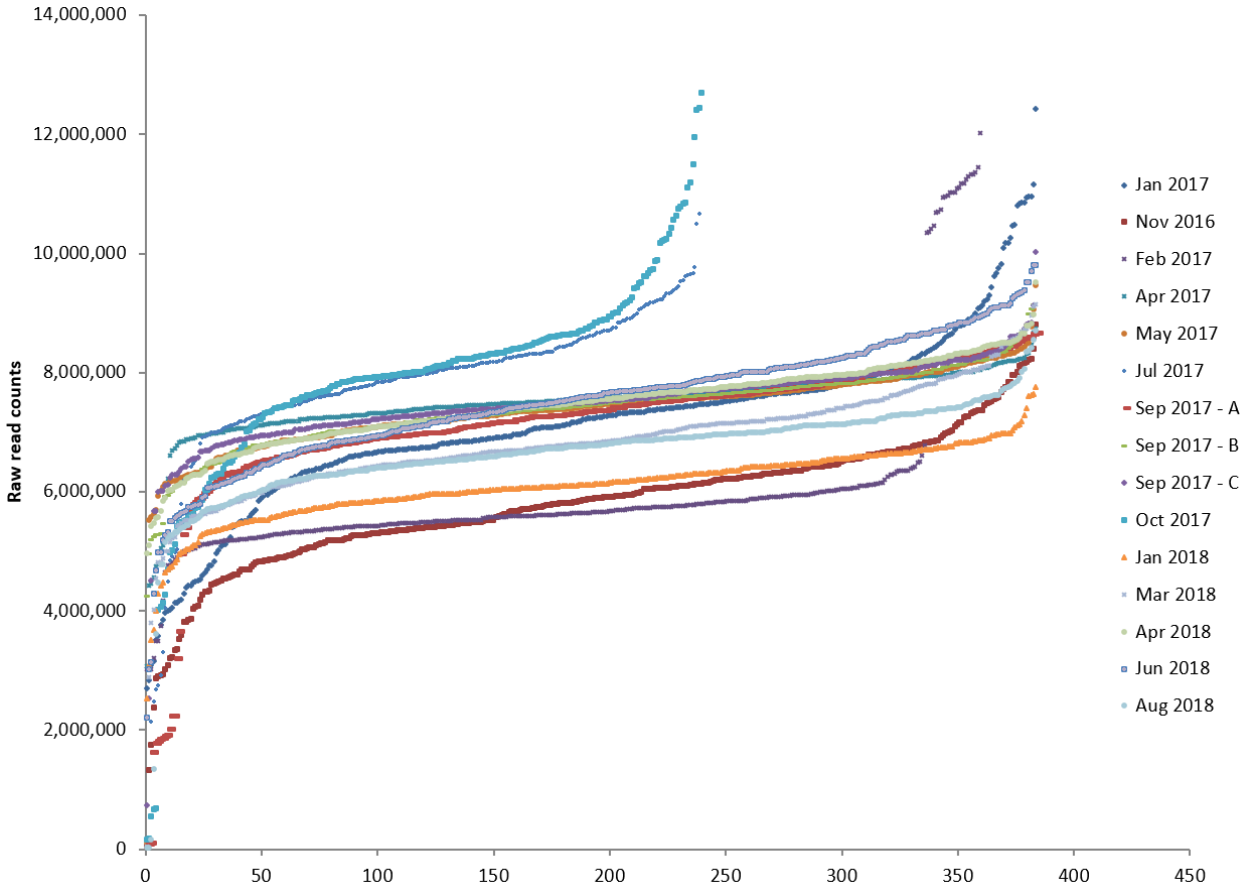

Figure S5. FASTQC results pre- and post-filtering with Cutadapt.

FASTQC results are from a single sample from the original set of 96 HS samples prepared in 12-plex and sequenced on the Illumina HiSeq 2500 with 125bp reads.

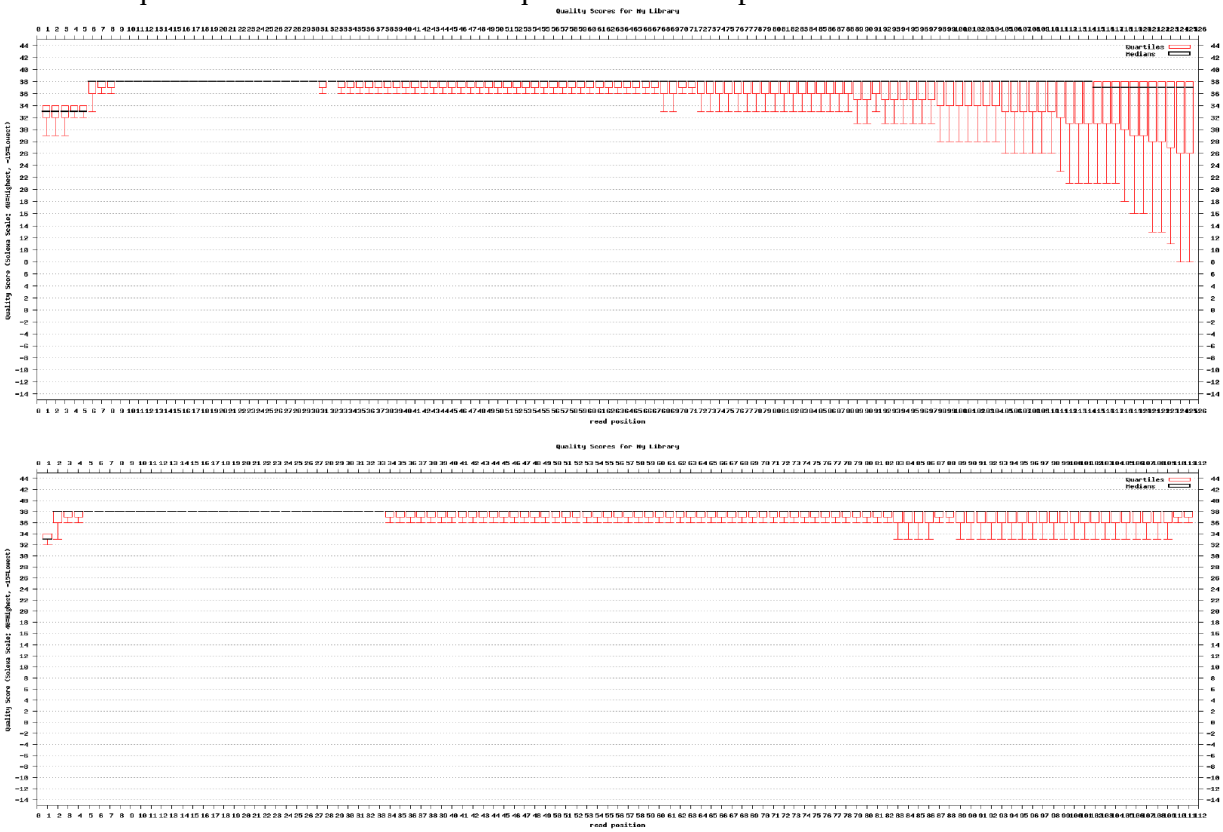

Figure S6. Overlap of called SNPs with known variants after read trimming with FASTX or Cutadapt.

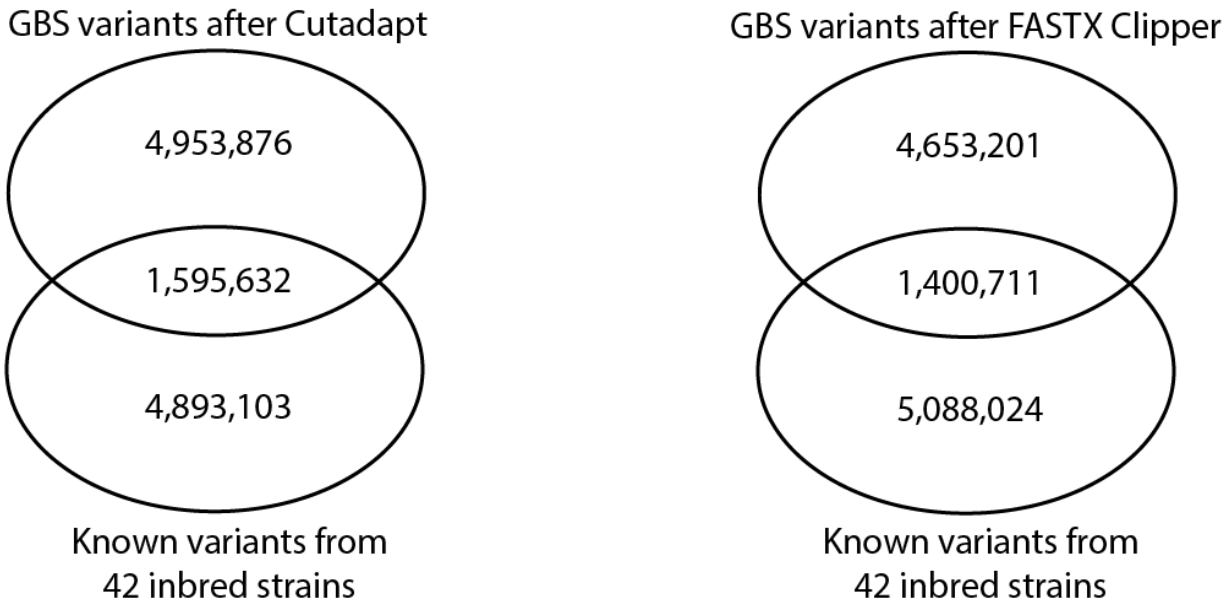

Figure S7. Number of variants by genotype discordance rates for 4 ANGSD genotype likelihood models.

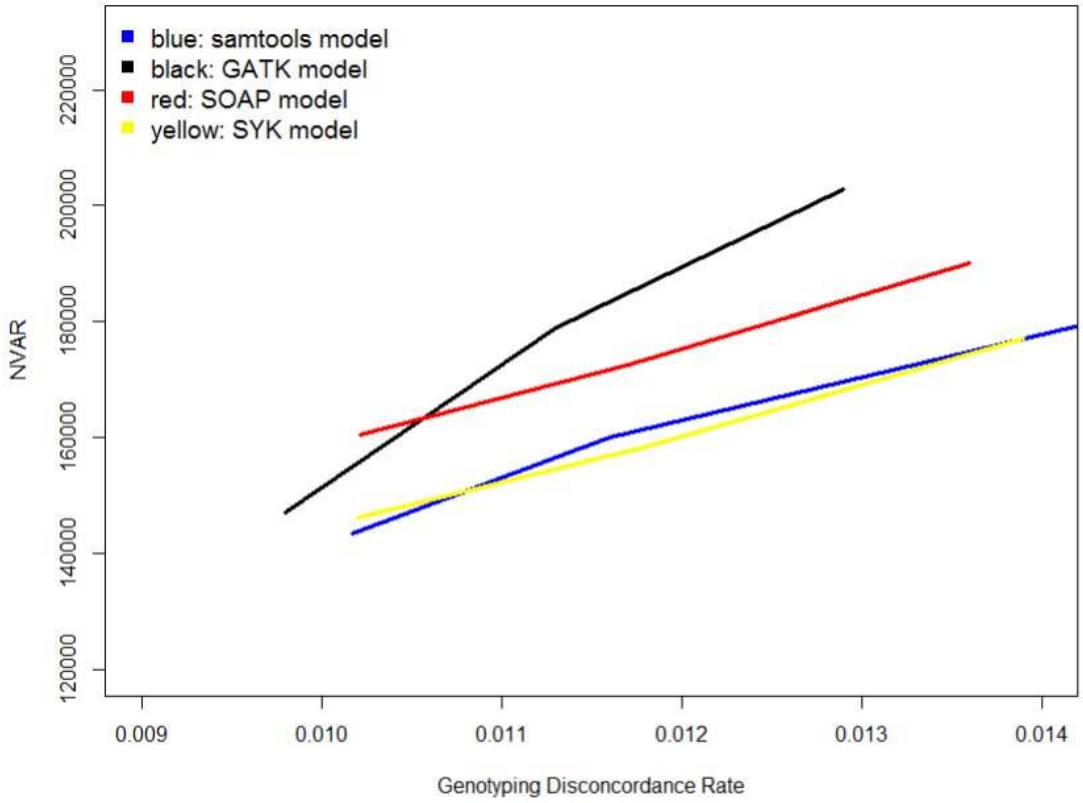

Figure S8. Available rat genetic maps.

Plotted physical and genetic distances are for chromosome 12.

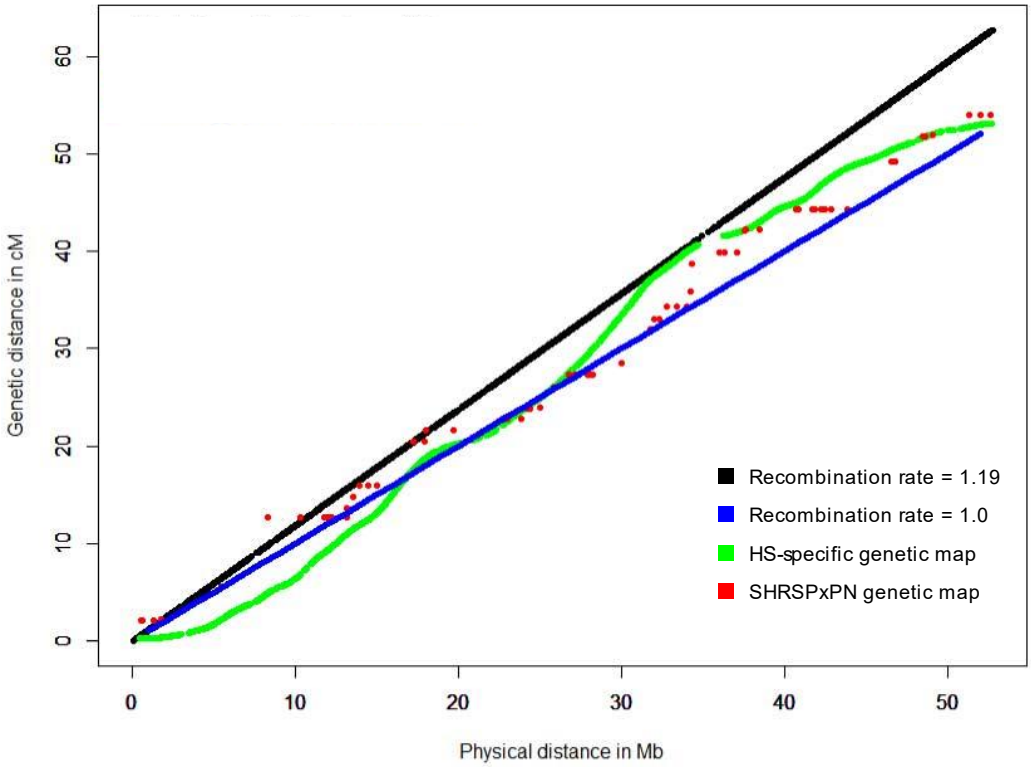

Table S1. Demultiplexing performance.

All methods began with the same number of reads from the original FASTQ. Final read and base pair counts are from after the reads have been trimmed of adapter, barcode, and restriction site sequences, as well as low-quality base pairs (< Q20).

	In-house Python Script	**GBSX**	**FASTX Barcode Splitter**
Reads with NlaIII adapter sequence	545,177 (3.07%)	475,581 (2.67%)	547,697 (3.07%)
Total bps processed	2,061,523,464	2,116,436,361	2,227,542,500
Total bps written to file	2,059,714,312	2,114,841,934	2,225,724,833
Proportion of bps retained	99.91%	99.92%	99.92%
Reads post-processing	17,771,754	17,786,280	17,820,340

Table S2. Comparison of variants calls after filtering with FASTX vs Cutadapt.

Data shown comes from the original set of 96 HS samples prepared in 12-plex and sequenced on the Illumina HiSeq 2500. At this step of pipeline optimization, variants were called utilizing GATK UnifiedGenotyper. Calls were unfiltered.

	FASTX Clipper	**Cutadapt**
Number of variants	6,075,821	6,581,115
Genotyping call rate	0.17	0.19
Mean minor allele count	3.96	4.25
Mean minor allele frequency	0.15	0.15
Number of singletons	433,960	548,975
Number monomorphic sites	807,453	773,074
Transition/transversion ratio	2.32	2.40
$T_I T_V$ ratio for singletons	3.23	3.40
Mean variant read depth	109.56	126.35
Mean quality score	601.79	715.56

Table S3. Variant metrics resulting from reads filtered at different mapping quality thresholds.

Data shown comes from the original set of 96 HS samples prepared in 12-plex and sequenced on the Illumina HiSeq 2500. Variants were called utilizing the SAMtools model and the -minMapQ filter in ANGSD. Calls were unfiltered.

	MAPQ = 20	**MAPQ = 30**	**MAPQ = 45**	**MAPQ = 60**	**MAPQ = 90**
Number of variants	372,860	372,330	363,790	316,949	233,322
Genotyping call rate	0.64	0.64	0.64	0.61	0.75
Mean minor allele count	5.96	5.96	6.06	5.86	7.36
Mean minor allele frequency	0.18	0.18	0.18	0.18	0.19
Number of singletons	16,781 (4.50%)	16,732 (4.49%)	16,550 (4.55%)	17,352 (5.47%)	11,773 (5.05%)
Number of monomorphic sites	122,478 (32.85%)	122,188 (32.82%)	116,738 (32.09%)	100,074 (31.57%)	56,179 (24.08%)
Transition/transversion ratio	1.23	1.24	1.26	1.31	1.41
$T_I T_V$ ratio for singletons	1.27	1.28	1.28	1.31	1.38
Mean variant read depth	157.78	157.73	159.25	152.48	188.80
Mean quality score	2,547	2,548	2,556	2,461	2,954

Table S4. Transition/transversion ratio before and after known sites filtering.

The presented data comes from ANGSD/Beagle variant calls for 3,601 HS samples, prior to imputation with IMPUTE2. Known SNPs came from both the 42 inbred genomes from Hermsen et. al 2015 (Hermsen et al. 2015) and the 8 inbred HS founder strains sequenced by the University of Michigan (Ramdas et al. 2018).

	Unfiltered SNPs	**Filtered for known SNPs**
AC	15,157	9,166
AG	888,657	42,275
AT	15,432	7,610
CG	18,043	8,061
CT	893,653	41,938
GT	15,118	9,177
$\mathbf{T_S}$	1,782,310	84,213
$\mathbf{T_V}$	63,750	34,014
$\mathbf{T_S T_V}$	27.96	2.48
Total # SNPs	1,846,060	118,227

Table S5. Imputation accuracy for chromosome 12 across different genetic maps.

The number of variants used for the concordance check is dependent on the overlap of the imputed variants with array data for the 96 HS rats with array genotypes. The MAF filter only removes monomorphic sites within the 96 HS rat sample used for the concordance check.

	cM/Mb = 1.00	**cM/Mb = 1.16**	**SHRSPxPN**	**HS-specific**
Number of variants before QC	158,452	158,452	158,452	158,452
Genotyping rate before QC	0.94	0.92	0.92	0.92
Variant removed for missingness > 10%	22,217	28,959	28,356	28,858
Variants removed for MAF < 0.005	50,380	61,270	61,592	59,812
Variants removed for HWE < $1x10^{-10}$	53	56	57	56
Number of variants after QC	85,802	68,167	68,447	69,726
Genotyping rate after QC	0.93	0.91	0.92	0.91
Number of variants in concordance check	5,912	5,590	5,594	5,646
Discordance rate	0.095	0.011	0.011	0.010